1 **Characterization of Type-2 Diacylglycerol Acyltransferases in the Green Microalga**

2 ***Chromochloris zofingiensis***

3

4 Yang Xu,[†] Lucas Falarz,[†,‡] Guanqun Chen [*,†,‡]

5

6 [†]Department of Agricultural, Food and Nutritional Science, University of Alberta, Edmonton,

7 Alberta, Canada, T6G 2P5

8

9 [‡]Department of Biological Sciences, University of Manitoba, Winnipeg, Manitoba, Canada, R3T

10 2N2

11

12

13 *Corresponding author. E-mail: gc24@ualberta.ca. Phone: +1 780 4923148. Fax: +1 780

14 4924265

15

ABSTRACT:

Diacylglycerol acyltransferase (DGAT) catalyzes the last and committed step of the acyl-CoA-dependent TAG biosynthesis and thus is a key target for manipulating oil production in microalgae. The microalga *Chromochloris zofingiensis* can accumulate substantial amounts of triacylglycerol (TAG) and represents a promising source of algal lipids. In this study, *C. zofingiensis DGAT2*s (*CzDGAT2*s) were characterized with *in silico*, *in vivo* (yeast) and *in vitro* assays. Putative CzDGAT2s were identified and their functional motifs and evolutionary relationship with other DGAT2s were analyzed. When *CzDGAT2*s were individually expressed in a TAG-deficient *Saccharomyces cerevisiae* strain, only *CzDGAT2C* could restore the TAG biosynthesis. Further *in vitro* assays indicated that CzDGAT2C displayed typical DGAT activity, which was fitted to the Michaelis-Menten equation, and N- and C-terminals were important for the enzyme activity. In addition, membrane yeast two-hybrid assay revealed a possible DGAT2 activity modulation via the formation of homodimer/heterodimer among different DGAT2 isoforms.

INTRODUCTION

Triacylglycerol (TAG), consisting of three fatty acids esterified to a glycerol backbone, is a major form of energy and carbon reservoir in many microalgal species and higher plants. TAG also plays crucial roles in the development and stress responses of these organisms. [1–3] Besides the important physiological functions, TAG is of great nutritional and industrial value and has been widely used as food, feed and renewable feedstock for various industrial applications. The ballooning population and increasing reliance on TAG-derived chemicals has resulted in the rising demands for vegetable oil. Microalgae have emerged as a promising source of lipids and have great potential to help meet the demands. Indeed, many microalgae can accumulate large amounts of TAG under adverse environmental conditions and have no competition with food crops for arable land. [4,5]

The green microalga *Chromochloris zofingiensis*, previously known as *Chlorella zofingiensis*, is a unicellular microalga with important industrial potential. [6] *C. zofingiensis* can accumulate a substantial amount (~27% dry cell weight) of storage TAG under adverse growth conditions. [7,8] In concert with TAG accumulation, *C. zofingiensis* also produces a red-color carotenoid pigment astaxanthin (~1-7 mg/g dry cell weight), which is mainly stored together with TAG in lipid bodies. [9] Astaxanthin has high nutritive value in food and feed industries due to its antioxidant and anti-inflammatory properties. [9] In addition, *C. zofingiensis* can grow quickly under phototrophic, heterotrophic and mixtrophic conditions and accumulate a large amount of biomass in a short period. [9] Therefore, *C. zofingiensis* is considered a promising source of lipids and natural astaxanthin. In this regard, understanding the metabolic pathways of lipid biosynthesis is pivotal for improving TAG production in *C. zofingiensis.*

In microalgae and higher plants, TAG is synthesized via the acyl-CoA dependent and

57   independent pathways. [2,5] In the acyl-CoA-dependent TAG biosynthesis, acyl-CoA :

58   diacylglycerol acyltransferase (DGAT, EC 2.3.1.20) catalyzes the final acylation of *sn*-1,2-

59   diacylglycerol and acyl-CoA to produce TAG. DGAT plays a determinant role in affecting the

60   flux of carbon into oil and thus has been regarded as the key target in numerous studies to

61   manipulate oil production. Plants and microalgae have two major forms of membrane-bound

62   DGAT, designated DGAT1 and DGAT2, which share no sequence homology. In plants, DGAT1

63   is likely to primarily contribute to oil accumulation whereas DGAT2 appears to be important for

64   the enrichment of unusual fatty acids in TAG. [10–13] Noticeably, recent studies revealed that many

65   microalgae contain one copy of DGAT1 and multiple copies of DGAT2, and DGAT2s play

66   important roles in algal lipid biosynthesis. [14–16] However, the physiological roles of DGAT1 and

67   DGAT2, as well as the exact contributions of different DGATs in lipid biosynthesis, are yet to be

68   extensively explored in microalgae. As a promising oleaginous microalgal species with high

69   industrial value, *C. zofingiensis* has been studied from both food science and physiology

70   perspectives, and its genome was just recently sequenced. [6] However, DGATs have not been

71   characterized in *C. zofingiensis*, which hampers the exploration of its potential in lipid

72   production. Thus, it is interesting to identify and characterize *C. zofingiensis* DGAT2s

73   (CzDGAT2s), which would be used in improving oil production in *C. zofingiensis* and other

74   microalgal species.

75   Here, we put forward *in silico* analysis, *in vivo* (yeast) and *in vitro* characterization to

76   explore the possible function of CzDGAT2s. Putative *CzDGAT2*s were identified from the *C.*

77   *zofingiensis* genome and were further characterized in *Saccharomyces cerevisiae* H1246, a

78   quadruple mutant devoid of TAG biosynthesis. The ability of each CzDGAT2 to restore TAG

79   biosynthesis of the yeast mutant was accessed and the *in vitro* DGAT activity was subsequently

80 examined using yeast microsomal fractions containing recombinant enzyme and the radiolabeled

81 substrate. The possible protein-protein interactions among different CzDGAT2 isoforms were

82 further tested using membrane yeast two-hybrid assay.

83

84 **MATERIALS AND METHODS**

85

86 **Identification of *CzDGAT2* Genes and Sequence Analysis**

87   To identify putative CzDGAT2s, a BLAST analysis was performed against the recently

88 published *C. zofingiensis* genomic database (v.5.2.3.2;

89 https://phytozome.jgi.doe.gov/pz/portal.html#!info?alias=Org_Czofingiensis_er; accessed on 09

90 August 2018) [6] with *Arabidopsis thaliana* DGAT2 (AtDGAT2) and *Chlamydomonas reinhardtii*

91 DGAT2s (CreDGAT2s) as the protein queries. Multiple sequence alignments of DGAT2 proteins

92 were conducted using ClustalW with the default settings in MEGA7 software. [17] As for

93 phylogenetic analysis, a neighbor-joining tree was built using the *Poisson* model and pairwise

94 deletion with 1000 bootstrap repetitions in the same software. Intron and exon distribution of

95 putative *CzDGAT2s* was analyzed using Gene Structure Display Server 2.0

96 (http://gsds.cbi.pku.edu.cn; accessed on 09 August 2018). [18] The topology prediction of

97 CzDGAT2 proteins was conducted using TMHMM [19] and Phobius (http://phobius.sbc.su.se/;

98 accessed on 08 December 2018). The theoretical molecular mass and isoelectric point values of

99 the deduced CzDGAT2 proteins were calculated on the Compute pI/Mw server

100 (http://web.expasy.org/compute_pi/, accessed on 09 August 2018). The sequence logos were

101 generated on signature motifs using WebLogo (http://weblogo.berkeley.edu/logo.cgi, accessed on

102   09 August 2018). [20]

103

Construction of Yeast Expression Vectors and Heterologous Expression of *CzDGAT2*s in

Yeast Mutant H1246

106   The coding sequences of *CzDGAT2*s were chemically synthesized (General Biosystems,

107   Morrisville, NC), and subcloned into the yeast expression pYES2 vector (Invitrogen, Burlington,

108   Canada), respectively, under the control of the galactose-inducible *GAL1* promoter. N- and C-

109   terminal truncation mutants of *CzDGAT2C* were PCR-amplified using primers F1 and R1, and

110   F2 and R2, respectively, and subcloned into the pYES2.1 vector. Primer sequences (restriction

111   sites are bold and underlined): F1, 5'-

112   GCAGA**GCGGCCGC***GAA*ATGCAGCTCCTTGCCGGTGCT-3'; R1, 5'-

113   TAT**GTCGAC**TCTGATGAATAGCTGCATGTCAG-3'; F2, 5'-

114   GCAGA**GCGGCCGC***GAA*ATGAAGGACGCGGTAGCA-3'; R2, 5'-

115   TAT**GTCGAC**GTCCAGGTGCTCTTGAACCA-3'. The integrity of each construct was

116   confirmed by sequencing. The constructs were then heterologously expressed in the *S. cerevisiae*

117   strain H1246, a quadruple mutant devoid of TAG synthesizing ability with the method described

118   in our previous study. [21,22] In brief, yeast transformation was performed using the *S.c.* EasyComp

119   Transformation Kit (Invitrogen). Transformants were selected on the solid minimal medium

120   lacking uracil which contained 0.67% (w/ v) yeast nitrogen base, 0.2 % (w/v) synthetic complete

121   medium lacking uracil (SC-Ura), 2% (w/v) dextrose, and 2% (w/v) agar. Successful

122   transformants were grown in liquid minimal medium containing 0.67% (w/v) yeast nitrogen base,

123   0.2 % (w/v) SC-Ura and 2% (w/v) raffinose, which were then used to inoculate the induction

124   medium containing 0.67% (w/v) yeast nitrogen base, 0.2 % (w/v) SC-Ura, 2% (w/v) galactose

6

125 and 1% (w/v) raffinose at an initial OD_{600} value of 0.4. For fatty acid feeding experiment, yeast

126 cells were cultured in induction medium with supplementation of 200 mM of linoleic acid

127 $(18:2\Delta^{9cis,12cis})$, α-linolenic acid $(C18:3\Delta^{9cis,12cis,18cis})$, or γ-linolenic acid $(C18:3\Delta^{6cis,9cis,12cis})$. The

128 yeast strains were grown at $30^{o}C$ with shaking at 220 rpm.

129

130 **Yeast Lipid Extraction and Analysis**

131 Total lipids were extracted from approximately 30 mg of lyophilized yeast cells using the method

132 described in our previous study. [13] One-hundred microgram of triheptadecanoin (C17:0 TAG)

133 were added to each sample as the internal standard. The extracted lipids were further separated

134 on a thin-layer chromatography (TLC) plate (0.25 mm Silica gel, DC-Fertigplatten, Macherey-

135 Nagel, Germany) with the developing solvent composed of hexane/diethyl ether/acetic acid

136 (80:20:1, v/v/v). The corresponding TAG bands were visualized by spraying with 0.05%

137 primulin (w/v) in acetone/water (80:20, v/v). The TAG bands were then scraped and

138 transmethylated by incubating with 1 mL of 3 N methanolic HCl at 80°C for 1 h. The resulting

139 fatty acid methyl esters were analyzed by GC-MS (Agilent Technologies, Wilmington, DE)

140 equipped with a capillary DB-23 column (30 m×0.25 mm×0.25 µm) as described previously. [13]

141

142 **Microsomal Fraction Preparation**

143   Microsomal fractions containing recombinant CzDGAT2s were extracted from yeast cells

144 as described previously. [13] Briefly, the recombinant yeast cells were collected at the mid-log

145 growth phase (OD_{600} value of ~6.5), washed and then resuspended in 1 mL of lysis buffer

146 containing 20 mM Tris-HCl (pH 7.9), 10 mM $MgCl_2$, 1 mM EDTA, 5% (v/v) glycerol, 300 mM

147 ammonium sulfate and 2 mM dithiothreitol. For microsomal fraction preparation, the yeast cells

7

148   were homogenized by a bead beater (Biospec, Bartlesville, OK) in the presence of glass beads

149   (diameter = 0.5 mm) and then centrifuged for 30 min at 10 000 g to sediment cell debris and

150   glass beads. The supernatant was further centrifuged at 105 000 g for 70 min to pellet the

151   microsomal fractions. The resulting microsomal pellet was then resuspended in 3 mM imidazole

152   buffer (pH 7.4) containing 125 mM sucrose and stored in aliquots at -80°C before use. The

153   above-mentioned procedures were all conducted at 4°C. The protein concentration was

154   quantified using the Bradford assay with BSA as the standard. [23]

155

156   ***In vitro* DGAT Assay**

157   DGAT assay was conducted as described previously. [22] The 60-µL reaction mixture had a

158   final composition of 200 mM HEPES-NaOH (pH 7.4), 3.2 mM MgCl$_2$, 333 µM *sn*-1,2-diolein

159   dispersed in 0.2% (v/v) Tween 20, and 15 µM [1-^{14}C] oleoyl-CoA (55 µCi/µmol) (PerkinElmer,

160   Waltham, MA). The reaction was initiated by adding 10 µg microsomal protein and further

161   incubated at 30°C with shaking for 1 h. The reaction was terminated by the addition of 10 µL of

162   SDS (10%, w/v). The entire reaction mixture was loaded on a TLC plate (0.25 mm Silica gel,

163   DC-Fertigplatten), which was developed in hexane/diethyl ether/acetic acid (80:20:1, v/v/v). The

164   corresponding TAG spots were visualized by phosphor imaging (Typhoon Trio Variable Mode

165   Imager, GE Healthcare, Chicago, IL) and their radioactivities were quantified on a LS 6500

166   multi-purpose scintillation counter (Beckman-Coulter, Brea, CA).

167

168   **Membrane Yeast-Two Hybrid Assay**

169   Protein-protein interactions between CzDGAT2s were tested using membrane yeast two-

170 hybrid system, which was kindly provided by Dr. Igor Stagljar, University of Toronto, with the

171 method described previously. [24] Briefly, individual cDNAs encoding CzDGAT2s were amplified

172 by PCR and cloned into the pBT3N bait vector or pPR3N prey vector, respectively. The resulting

173 pBT3N:bait and pPR3N:prey or control prey (Ost-N_{ub}I 'positive' control prey or Ost-N_{ub}G

174 'negative' control prey) were co-transformed into a yeast strain NMY51 (*MATa, his3Δ200, trp1-*

175 *901, leu2- 3,112, ade2, LYS2::(lexAop)4-HIS3,ura3::(lexAop)8-lacZ,ade2::(lexAop)8-ADE2,*

176 *GAL4*). Yeast cells expressing each bait/prey combination were first selected on synthetic drop-

177 out (SD) agar plates lacking Leu and Trp to ensure the presence of both bait and prey vectors.

178 The possible protein-protein interaction was then assayed on SD agar plates lacking Ade, His,

179 Leu and Trp using 1: 10 serial dilution of cell cultures starting from an OD600 value of 0.4.

180

181 **RESULTS AND DISCUSSION**

182

183 **Identification of Putative DGAT2s from *C. zofingiensis* and Phylogenetic Analysis, Gene**

184 **Structure and Membrane Topology Analysis of Putative CzDGAT2s.**

185   With the protein sequences of AtDGAT2 and CreDGAT2A, B, C, D and E as the queries,

186 seven putative CzDGAT2s were identified from the recently released *C. zofingiensis* genomic

187 database. [6] The general information on corresponding cDNAs and the encoded enzymes is listed

188 in Supplementary Table S1. The lengths of the cDNA and the encoded protein and the molecular

189 mass of CzDGAT2s varied substantially, ranging from 828 to 1311 bp, 267 to 437 amino acid

190 residues, and 31.1 to 48.9 kDa, respectively. Interestingly, all CzDGAT2s have maintained basic

191 calculated isoelectric points, ranging from 8.68 to 9.76, which is consistent with those of

9

192 DGAT2s from other species. [25]

193   To explore the evolutionary relationship of CzDGAT2s with their homologs in plants,

194 animals, yeast and green microalgae, a neighbor-joining tree was constructed using the protein

195 sequences of CzDGAT2s and those from the model plant, animal, yeast and microalgal species

196 including *A. thaliana* (AtDGAT2), *Linum usitatissimum* (LuDGAT2), *Homo sapiens* (HsDGAT2),

197 *Mus musculus* (MmDGAT2), *S. cerevisiae* (ScDGAT2) and *C. reinhardtii* (CreDGAT2s). As

198 shown in Figure 1, CzDGAT2s were separated into three groups, with CzDGAT2C grouping

199 with AtDGAT2, LuDGAT2 and CreDGAT2A (plant-like group), CzDGAT2F and G grouping

200 with HsDGAT2, MmDGAT2, ScDGAT2 and CreDGAT2B (animal/fungus-like group), and the

201 remaining CzDGAT2s and CreDGAT2s falling into another group (algae group). The divergent

202 distribution of CzDGAT2s was consistent with that in other green microalgal species, such as *C.*

203 *reinhardtii* and *Coccomyxa sp.* C-169. [14] A comprehensive phylogenetic analysis of DGAT2 from

204 different green microalgal species confirmed that green algal DGAT2 appears to be highly

205 divergent from each other and among the isoforms from the same species (Supplementary Figure

206 S1). All the studied green algae contain one DGAT2 closely related to higher plant DGAT2

207 (plant-like group), at least one DGAT2 with homologies to animal and fungal DGAT2

208 (animal/fungus-like group), and others that are different from either of the above-mentioned

209 eukaryotic forms.

210   The structures of *CzDGAT2* genes and the predicted transmembrane domains of the

211 encoded proteins, were subsequently analyzed and compared with their homologs (Figure 1 and

212 Supplementary Figure S2). Diverse structures were found among microalgal *DGAT2* genes,

213 ranging from 1 to 7 and 6-13 exons in CzDGAT2s and CreDGAT2s, respectively, which are

214 different to the similar exon numbers in DGAT2s from *A. thaliana* (8-9 exons, Figure 1) and

10

215   other terrestrial plants. [26] In terms of the membrane topology, CzDGAT2A, B, C, and E were

216   predicted to contain 1 to 3 transmembrane domains, which is consistent with the observations

217   from other DGAT2s. [26] Although no transmembrane domain was predicted in CzDGAT2D, F and

218   G using TMHMM (Figure 1), these enzymes were predicted to possess 2-4 transmembrane

219   domains in TMPred (https://embnet. vital-it.ch/software/TMPRED_form.html, accessed on 18

220   Oct 2018). Indeed, the prediction results of membrane protein topology vary among different

221   prediction algorithms. [26] Thus far, the topology structures of DGAT2 have been experimentally

222   determined for mouse and *S. cerevisiae* DGAT2s using protease protection assays and chemical

223   modification, respectively. [26,27] Such methods would be used to reveal the topology structures of

224   the diverse algal DGAT2s.

225

226   **Functional Motif Analysis of CzDGAT2s.**

227   The conserved motifs with functional importance in CzDGAT2 were further analyzed

228   (Figure 2). As shown in Figure 2A, although the FLXLXXXn (n=non polar amino acid) motif in

229   the mouse DGAT2, as well as its corresponding FVLF motif in ScDGAT2, have been proposed

230   to be a putative lipid binding motif, [27,28] this region was not conserved among CzDGAT2s and

231   CreDGAT2s (Figure 2A).The YFP motif is conserved among DGAT2s from animals and plants,

232   and is essential for DGAT2 activity. [27] This motif was found to be highly conserved among

233   CzDGAT2s and CreDGAT2s from the plant-like and animal/fungus-like groups, including

234   CzDGAT2C, CzDGAT2G, CreDGAT2A, and CreDGAT2B, but not found in the DGAT2s

235   belonging to the algae group (Figure 2B). The putative CzDGAT2s from the algae group only

236   have the conserved YF motif with the third residue tending to change from Pro to a hydrophilic

237   amino acid (Figure 2B).

238   Another functionally important motif in DGAT2 is the HPHG motif, which was proposed

239   to partially consist of the active site. [27,28] The HPHG motif is conserved among animal and

240   fungal DGAT2s and the equivalent EPHS motif is conserved among plant DGAT2s, [27] whereas

241   the putative CzDGAT2s have large variations in the conservation degrees of this motif (Figure

242   2C). Only CzDGAT2C and CzDGAT2G from the plant-like and animal/fungus-like DGAT

243   groups, respectively, have the conserved EPHS and HPHG motifs. The other CzDGAT2s,

244   however, have a more animal/fungus-like F/YPHG sequence. On the contrary, the motif

245   RXGFX(K/R)XAXXXGXX(L/V)VPXXXFG(E/Q) is the longest conserved sequence in plant

246   and animal DGAT2s, which is also present in CzDGAT2s (Figure 2D). Nevertheless, it would be

247   interesting to explore the functional importance of the putative functional motifs of algal

248   DGAT2s using mutagenesis in the future.

249

250   **The Functions of CzDGAT2s in Recovering Lipid Biosynthesis in Yeast Mutant H1246.**

251   To further characterize the putative CzDGAT2s, the cDNAs encoding 5 representative

252   CzDGAT2s from the three DGAT2 groups (Figure 1), including CzDGAT2A, B, C, D, and F,

253   were synthesized and heterologously expressed in the yeast mutant H1246. The yeast cells

254   hosting *CzDGAT2*s were cultured in the induction medium for 48 h and harvested for lipid

255   analysis. Only CzDGAT2C was able to recover TAG biosynthesis of the yeast strain (Figure 3A),

256   suggesting that *CzDGAT2C* encoded an active enzyme. The TAG bands were extracted from the

257   TLC plates and analyzed by GC-MS. The results confirmed that the yeast producing CzDGAT2C

258   generated higher amount of TAG than the negative control (Figure 3B). Although other

259   CzDGAT2s produced very weak TAG bands on the TLC plate, the subsequent analysis on GC-

260   MS indicated that the formed TAGs were very low and had no significant difference to the

12

261   negative control.

262   The TAG content of yeast producing CzDGAT2C was further accessed by feeding the

263   yeast cultures with exogenous fatty acids including, linoleic acid, α-linolenic acid, and γ-

264   linolenic acid. As shown in Figure 3C and 3D, CzDGAT2C could incorporate linoleic acid rather

265   than the other two fatty acids into yeast TAG, suggesting that CzDGAT2C might contribute to the

266   production of TAG with linoleic acid in *C. zofingiensis*. Indeed, *C. zofingiensis* contains ~20% of

267   linoleic acid in TAG. [29] On the contrary, when the yeast cells producing other DGAT2 candidates

268   were fed with those exogenous fatty acids, no TAG was produced (data not shown), which was

269   consistent with the results in Figure 3A.

270   CzDGAT2C, belonging to the plant-like DGAT2 group, shares homologies to AtDGAT2

271   (36.9% pairwise identity) and CreDGAT2A (47.7% pairwise identity). In this group, neither

272   native AtDGAT2 nor CreDGAT2A could complement the TAG deficient phenotype of yeast

273   mutant H1246, [16,30] although their functions in lipid biosynthesis have been proved by transit

274   expressing *AtDGAT2* in *Nicotiana benthamiana* leaves, [31] by expressing a yeast codon-optimized

275   *AtDGAT2* in yeast, [32] and by over-expressing *CreDGAT2A* in *C. reinhardtii.* [33] It is possible that

276   the codon usage is different among yeast, algae and plants, and thus the accumulation of these

277   DGAT2s in yeast was too low to actively catalyze the biosynthesis of TAG. However, many

278   papers reported that the expression of native algal DGAT2s, including those from green

279   microalgae with close evolutionary relationship with *C. zofingiensis*, could restore TAG

280   biosynthesis in the yeast strain H1246. [15,16] Therefore, codon-usage might be partially the reason

281   of the low TAG content in the yeast strain hosting CzDGAT2C in this study (Figure 3) and no

282   TAG accumulation in the yeast cells producing other CzDGAT2 isoforms.

283

284 ***In vitro* Characterization of DGAT Activity.**

285   To further test the activity of CzDGAT2C, yeast microsomal fractions containing

286 recombinant CzDGAT2C were prepared and used in *in vitro* DGAT assay. Consistent with the *in*

287 *vivo* results in yeast (Figure 3), CzDGAT2C displayed a weak but detectable DGAT activity

288 (Figure 4A). To kinetically characterize the CzDGAT2C, its activity was further examined over a

289 range of oleoyl-CoA concentrations. As shown in Figure 4B, CzDGAT2C had an activity

290 dependence on increasing oleoyl-CoA concentration: the DGAT activity rapidly enhanced with

291 the increase of oleoyl-CoA concentrations from 0 to 5 µM, and then increased slightly with

292 further increases in oleoyl-CoA concentration. The initial reaction velocity data of CzDGAT2C

293 were fitted to the Michaelis-Menten equation, and the apparent V_{max} and K_m value were 0.86

294 pmol TAG/ min/ mg protein and 3.07 µM oleoyl-CoA, respectively.

295   The apparent K_m value represents the DGAT affinity to its substrate acyl-CoA. The K_m

296 value obtained for CzDGAT2C is close to the previously characterized K_m values for DGAT1

297 from a few plant species, including *Brasscia napus*, *Corylus americana*, and *Zea mays*, ranging

298 from 0.6 to 2.8 µM oleoyl-CoA. [22,34,35] It should be noted that the K_m values of DGAT differed

299 largely among publications, perhaps due to the differences in enzyme types/sources and reaction

300 conditions, ranging from 0.6-2.8 µM oleoyl-CoA for plant DGAT1s, [22,34,35] 8.3 µM oleoyl-CoA

301 for mammalian DGATs, [36] 13-19.4 µM oleoyl-CoA for fungal DGAT2, [37] to 26-667 µM oleoyl-

302 CoA or palmitoleoyl-CoA for bacteria DGAT. [38–40] Indeed, K_m value of plant DGAT appears to

303 markedly vary from those of heterotrophic organisms, which likely have more abundant energy

304 and carbon supply for oil storage. [35] Moreover, these kinetic studies of DGAT mainly used

305 microsomal protein. Although our previous work on the purified DGAT1 from *Brassica napus*

306 showed similar kinetic parameters to the crude yeast microsomal preparation [22, 34], it would still

307 be interesting to purify the CzDGAT2C for additional kinetic studies in the future. The purified

308 enzyme would not be potentially affected by other proteins in the microsomal preparation but

309 might be influenced by the detergents to solubilize the enzyme.

310   Based on the TMHMM prediction, CzDGAT2C contains a short N-terminal hydrophilic

311 tail (3 amino acid), followed by 2 adjacent transmembrane domains (positions 4-23 and 30-52)

312 and a large C-terminal hydrophilic fragment (Figure 4C), whereas Phobius predicts CzDGAT2C

313 with only one transmembrane domain (position 38-57) connecting a small N-terminal and a large

314 C-terminal hydrophilic tails. To further explore the role of the N- and C-termini in CzDGAT2C

315 function, truncation mutagenesis was carried out. Removal of the first 23 amino acid residues in

316 the N-terminus (variant 24-316) and the last 27 amino acid residues in the C-terminus (variant 1-

317 289) resulted in large decreases in DGAT activity (Figure 4D), suggesting that both the N- and

318 C-termini of CzDGAT2 are important and sensitive to modifications. Similar observations have

319 also been reported in ScDGAT2.[27]

320

321 **Probe Potential Protein-protein Interaction Among CzDGAT2s Using Membrane Yeast**

322 **Two-hybrid Assay.**

323   To explore the potential protein-protein interactions among CzDGAT2s, CzDGAT2A, B,

324 C, D, and F was individually used as bait and prey and the interaction within each bait and prey

325 combination was tested using the split-ubiquitin membrane yeast two hybrid system. [24] Possible

326 interactions were only observed among CzDGAT2A, C and D (Figure 5). CzDGAT2C was found

327 to interact with CzDGAT2A and CzDGAT2D by using CzDGAT2C as bait and CzDGAT2A or D

328 as prey. These interactions were also observed when bait and prey were switched. Additionally,

329 self-interactions were observed for CzDGAT2A, C, and D (Figure 5), suggesting that these

330   enzymes might form multimeric complexes.

331   Protein-protein interaction has been proven to play important physiological roles in

332   various organisms. For instance, mouse DGAT2 could form homodimer and heterodimer with

333   mouse monoacylglycerol acyltransferase, which could promote TAG synthesis. [41,42] Similarly,

334   the physical interactions among CzDGAT2s may also be metabolically meaningful in *C.*

335   *zofingiensis*. Different CzDGAT2 isoforms may have different affinities and preferences for

336   substrate. The formation of homodimer and/or heterodimer of CzDGAT2s could potentially

337   result in a precise modulation of enzyme performance by controlling the composition of the

338   CzDGAT2 isoforms in the dimer, which may contribute to the stress tolerance and resistance of

339   *C. zofingiensis*. Indeed, transcriptomic analyses suggested that individual *CzDGAT2*s have

340   different expression patterns in response to stress. [6] Further experiments are required to explore

341   the contribution of the possible CzDGAT2 interactions to TAG biosynthesis and cell physiology

342   in *C. zofingiensis*, and the results would be valuable for manipulating DGAT2s to improve lipid

343   production in this promising oleaginous alga species.

344   DGAT has been characterized in many microalgal species, in which DGAT1, 2 and dual-

345   function DGAT have been shown to play crucial roles in algal TAG biosynthesis. [15, 33, 43, 44] The

346   current study provides the first functional characterization of DGAT2s from *C. zofingiensis*, a

347   promising source of lipids and natural astaxanthin for food and feed industries. The

348   comprehensive *in silico, in vivo* (yeast) and *in vitro* analysis, especially the evolutionary analysis,

349   enzymatic kinetics, functional motif analysis, N- and C-terminal analysis and protein-protein

350   interaction analysis, provide novel information about CzDGAT2 and expand our understanding

351   of algal DGAT2s.

352   In conclusion, putative CzDGAT2s were identified from *C. zofingiensis*, which could be

353 divided into three groups based on their phylogenetic relationship with DGAT2s from higher

354 plants, yeast and another green microalga. The function of the putative CzDGAT2s were further

355 tested using yeast mutant H1246 as a platform. CzDGAT2C, a homolog of AtDGAT2, was able

356 to recover TAG biosynthesis of the yeast mutant and its DGAT activity was confirmed via *in*

357 *vitro* enzyme assays. Possible physical interactions among CzDGAT2s were probed via

358 membrane yeast two-hybrid assay, suggesting a unique enzyme modulation might be present in

359 *C. zofingiensis*. Overall, our findings provide valuable information on CzDGAT2s, which could

360 be used as the foundation for further characterizing the properties and functions of CzDGAT2s,

361 exploring their interactions with the DGAT family and with other enzymes, and improving lipid

362 production in algae.

363

364 **ABBREVIATIONS USED**

365 DGAT, acyl-CoA : diacylglycerol acyltransferase; TAG, triacylglycerol; TLC, thin-layer

366 chromatography; SC-Ura, synthetic complete medium lacking uracil; SD, synthetic drop-out.

367

375 2016-05926) and the Canada Research Chairs Program.

376

CONFLICT OF INTEREST

378 The authors declare no conflict of interest.

379

APPENDIX A. SUPPLEMENTARY MATERIAL

381 Supplementary Table S1. Overview of putative *DGAT2* cDNAs identified in the *C. zofingiensis*

382 genomic database.

383 Supplementary Figure S1. Phylogenetic relationship among deduced amino acid sequences of

384 CzDGAT2s and DGAT2s from other organisms. *At*, *Arabidopsis thaliana*; *Cre, Chlamydomonas*

385 *reinhardtii; Cs, Coccomyxa_subellipsoidea; Hs, Homo sapiens*; *Lu*, *Linum usitatissimum*;

386 *Micromonas, Micromonas spRCC299; Mm, Mus musculus*; *Mp, Micromonas pusilla; No,*

387 *Nannochloropsis oceanica*; *Ol, Ostreococus lucimarinus*; *Sc, Saccharomyces cerevisiae; Vc,*

388 *Volvox carteri.* Bootstrap values for the neighbor-joining tree based on 1000 bootstrap repetitions

389 are shown at the tree nodes. Phytozome/Genbank accession number for each protein sequence is

390 shown in brackets.

391 Supplementary Figure S2. The gene structure of *DGAT2* from *Homo sapiens* (HsDGAT2) and

392 *Mus musculus* (MmDGAT2).

393

394

395

18

REFERENCES

(1) Hu, Q.; Sommerfeld, M.; Jarvis, E.; Ghirardi, M.; Posewitz, M.; Seibert, M.; Darzins, A. Microalgal Triacylglycerols as Feedstocks for Biofuel Production: Perspectives and Advances. *Plant J.* **2008**, *54* (4), 621–639.

(2) Xu, Y.; Caldo, K. M. P.; Pal-Nath, D.; Ozga, J.; Lemieux, M. J.; Weselake, R. J.; Chen, G. Properties and Biotechnological Applications of Acyl-CoA:Diacylglycerol Acyltransferase and Phospholipid:Diacylglycerol Acyltransferase from Terrestrial Plants and Microalgae. *Lipids* **2018**.

(3) Yang, Y.; Benning, C. Functions of Triacylglycerols during Plant Development and Stress. *Curr. Opin. Biotechnol.* **2018**, *49*, 191–198.

(4) Li-Beisson, Y.; Beisson, F.; Riekhof, W. Metabolism of Acyl-Lipids in *Chlamydomonas Reinhardtii*. *Plant J.* **2015**, *82* (3), 504–522.

(5) Kong, F.; Romero, I. T.; Warakanont, J.; Li-Beisson, Y. Lipid Catabolism in Microalgae. *New Phytol.* **2018**, *218* (4), 1340–1348.

(6) Roth, M. S.; Cokus, S. J.; Gallaher, S. D.; Walter, A.; Lopez, D.; Erickson, E.; Endelman, B.; Westcott, D.; Larabell, C. A.; Merchant, S. S.; et al. Chromosome-Level Genome Assembly and Transcriptome of the Green Alga *Chromochloris Zofingiensis* Illuminates Astaxanthin Production. *Proc. Natl. Acad. Sci. U. S. A.* **2017**, *114* (21), E4296–E4305.

(7) Mao, X.; Wu, T.; Sun, D.; Zhang, Z.; Chen, F. Differential Responses of the Green Microalga *Chlorella Zofingiensis* to the Starvation of Various Nutrients for Oil and Astaxanthin Production. *Bioresour. Technol.* **2018**, *249*, 791–798.

(8) Zhu, S.; Wang, Y.; Shang, C.; Wang, Z.; Xu, J.; Yuan, Z. Characterization of Lipid and

19

418   Fatty Acids Composition of *Chlorella Zofingiensis* in Response to Nitrogen Starvation. *J.*

419   *Biosci. Bioeng.* **2015**, *120* (2), 205–209.

420   (9)   Liu, J.; Sun, Z.; Gerken, H.; Liu, Z.; Jiang, Y.; Chen, F. *Chlorella Zofingiensis* as an

421   Alternative Microalgal Producer of Astaxanthin: Biology and Industrial Potential. *Mar.*

422   *Drugs* **2014**, *12* (6), 3487–3515.

423   (10)   Shockey, J. M.; Gidda, S. K.; Chapital, D. C.; Kuan, J.-C. C.; Dhanoa, P. K.; Bland, J. M.;

424   Rothstein, S. J.; Mullen, R. T.; Dyer, J. M. Tung Tree DGAT1 and DGAT2 Have

425   Nonredundant Functions in Triacylglycerol Biosynthesis and Are Localized to Different

426   Subdomains of the Endoplasmic Reticulum. *Plant Cell* **2006**, *18* (9), 2294–2313.

427   (11)   Kroon, J. T. M.; Wei, W.; Simon, W. J.; Slabas, A. R. Identification and Functional

428   Expression of a Type 2 Acyl-CoA:Diacylglycerol Acyltransferase (DGAT2) in Developing

429   Castor Bean Seeds Which Has High Homology to the Major Triglyceride Biosynthetic

430   Enzyme of Fungi and Animals. *Phytochemistry* **2006**, *67* (23), 2541–2549.

431   (12)   Li, R.; Yu, K.; Hatanaka, T.; Hildebrand, D. F. *Vernonia* DGATs Increase Accumulation of

432   Epoxy Fatty Acids in Oil. *Plant Biotechnol. J.* **2010**, *8* (2), 184–195.

433   (13)   Xu, Y.; Holic, R.; Li, D.; Pan, X.; Mietkiewska, E.; Chen, G.; Ozga, J.; Weselake, R. J.

434   Substrate Preferences of Long-Chain Acyl-CoA Synthetase and Diacylglycerol

435   Acyltransferase Contribute to Enrichment of Flax Seed Oil with α-Linolenic Acid.

436   *Biochem. J.* **2018**, *475*, 1473–1489.

437   (14)   Chen, J. E.; Smith, A. G. A Look at Diacylglycerol Acyltransferases (DGATs) in Algae. *J.*

438   *Biotechnol.* **2012**, *162*, 28–39.

439   (15)   Xin, Y.; Lu, Y.; Lee, Y.-Y. Y.; Wei, L.; Jia, J.; Wang, Q.; Wang, D.; Bai, F.; Hu, H.; Hu, Q.;

440   et al. Producing Designer Oils in Industrial Microalgae by Rational Modulation of Co-

441   Evolving Type-2 Diacylglycerol Acyltransferases. *Mol. Plant* **2017**, *10* (12), 1523–1539.

442 (16)   Liu, J.; Han, D.; Yoon, K.; Hu, Q.; Li, Y. Characterization of Type 2 Diacylglycerol

443   Acyltransferases in *Chlamydomonas Reinhardtii* Reveals Their Distinct Substrate

444   Specificities and Functions in Triacylglycerol Biosynthesis. *Plant J.* **2016**, *86* (1), 3-19.

445 (17)   Kumar, S.; Stecher, G.; Tamura, K. MEGA7: Molecular Evolutionary Genetics Analysis

446   Version 7.0 for Bigger Datasets. *Mol. Biol. Evol.* **2016**, *33* (7), msw054.

447 (18)   Hu, B.; Jin, J.; Guo, A. Y.; Zhang, H.; Luo, J.; Gao, G. GSDS 2.0: An Upgraded Gene

448   Feature Visualization Server. *Bioinformatics* **2015**, *31* (8), 1296–1297.

449 (19)   Krogh, A.; Larsson, B.; von Heijne, G.; Sonnhammer, E. Predicting Transmembrane

450   Protein Topology with a Hidden Markov Model: Application to Complete Genomes. *J.*

451   *Mol. Biol.* **2001**, *305* (3), 567–580.

452 (20)   Crooks, G.; Hon, G.; Chandonia, J.; Brenner, S. WebLogo: A Sequence Logo Generator.

453   *Genome Res.* **2004**, *14*, 1188–1190.

454 (21)   Sandager, L.; Gustavsson, M. H.; Stahl, U.; Dahlqvist, A.; Wiberg, E.; Banas, A.; Lenman,

455   M.; Ronne, H.; Stymne, S. Storage Lipid Synthesis Is Non-Essential in Yeast. *J Biol Chem*

456   **2002**, *277* (8), 6478–6482.

457 (22)   Xu, Y.; Chen, G.; Greer, M. S.; Caldo, K. M. P.; Ramakrishnan, G.; Shah, S.; Wu, L.;

458   Lemieux, M. J.; Ozga, J.; Weselake, R. J. Multiple Mechanisms Contribute to Increased

459   Neutral Lipid Accumulation in Yeast Producing Recombinant Variants of Plant

460   Diacylglycerol Acyltransferase 1. *J. Biol. Chem.* **2017**, *292* (43), 17819–17831.

461 (23)   Bradford, M. M. A Rapid and Sensitive Method for the Quantitation of Microgram

21

462   Quantities of Protein Utilizing the Principle of Protein-Dye Binding. *Anal. Biochem.* **1976**,

463   *72* (1–2), 248–254.

464   (24)   Snider, J.; Kittanakom, S.; Damjanovic, D.; Curak, J.; Wong, V.; Stagljar, I. Detecting

465   Interactions with Membrane Proteins Using a Membrane Two-Hybrid Assay in Yeast. *Nat.*

466   *Protoc.* **2010**, *5* (7), 1281–1293.

467   (25)   Cao, H. Structure-function Analysis of Diacylglycerol Acyltransferase Sequences from 70

468   Organisms. *BMC Res. Notes*, **2011**, *4*(1), 249.

469   (26)   Liu, Q., Siloto, R.M.P., Lehner, R., Stone, S.J. and Weselake, R.J. Acyl-CoA:

470   Diacylglycerol Acyltransferase: Molecular Biology, Biochemistry and Biotechnology.

471   *Prog. Lipid Res.*, **2012**, *51*(4), 350-377.

472   (27)   Liu, Q.; Siloto, R. M. P.; Snyder, C. L.; Weselake, R. J. Functional and Topological

473   Analysis of Yeast Acyl-CoA:Diacylglycerol Acyltransferase 2, an Endoplasmic Reticulum

474   Enzyme Essential for Triacylglycerol Biosynthesis. *J. Biol. Chem.* **2011**, *286* (15), 13115–

475   13126.

476   (28)   Stone, S. J.; Levin, M. C.; Farese, R. V. Membrane Topology and Identification of Key

477   Functional Amino Acid Residues of Murine Acyl-CoA:Diacylglycerol Acyltransferase-2.

478   *J. Biol. Chem.* **2006**, *281* (52), 40273–40282.

479   (29)   Liu, J.; Huang, J.; Sun, Z.; Zhong, Y.; Jiang, Y.; Chen, F. Differential Lipid and Fatty Acid

480   Profiles of Photoautotrophic and Heterotrophic *Chlorella Zofingiensis*: Assessment of

481   Algal Oils for Biodiesel Production. *Bioresour. Technol.* **2011**, *102* (1), 106–110.

482   (30)   Weselake, R. J.; Taylor, D. C.; Rahman, M. H.; Shah, S.; Laroche, A.; McVetty, P. B. E.;

483   Harwood, J. L. Increasing the Flow of Carbon into Seed Oil. *Biotechnol. Adv.* **2009**, *27* (6),

484 866–878.

(31) Zhou, X. R.; Shrestha, P.; Yin, F.; Petrie, J. R.; Singh, S. P. AtDGAT2 Is a Functional
    Acyl-CoA:Diacylglycerol Acyltransferase and Displays Different Acyl-CoA Substrate
    Preferences than AtDGAT1. *FEBS Lett.* **2013**, *587* (15), 2371–2376.

(32) Aymé, L.; Baud, S.; Dubreucq, B.; Joffre, F.; Chardot, T. Function and Localization of the
    Arabidopsis Thaliana Diacylglycerol Acyltransferase DGAT2 Expressed in Yeast. *PLoS*
    One **2014**, *9* (3), 1–9.

(33) Iwai, M.; Ikeda, K.; Shimojima, M.; Ohta, H. Enhancement of Extraplastidic Oil Synthesis
    in *Chlamydomonas Reinhardtii* Using a Type-2 Diacylglycerol Acyltransferase with a
    Phosphorus Starvation–inducible Promoter. *Plant Biotechnol. J.* **2014**, *12* (6), 808–819.

(34) Caldo, K. M. P.; Acedo, J. Z.; Panigrahi, R.; Vederas, J. C.; Weselake, R. J.; Lemieux, M. J.
    Diacylglycerol Acyltransferase 1 Is Regulated by Its N-Terminal Domain in Response to
    Allosteric Effectors. *Plant Physiol* **2017**, *175* (2), 667–680.

(35) Roesler, K.; Shen, B.; Bermudez, E.; Li, C.; Hunt, J.; Damude, H. G.; Ripp, K. G.; Everard,
    J. D.; Booth, J. R.; Castaneda, L.; et al. An Improved Variant of Soybean Type 1
    Diacylglycerol Acyltransferase Increases the Oil Content and Decreases the Soluble
    Carbohydrate Content of Soybeans. *Plant Physiol.* **2016**, *171* (2), 878–893.

(36) Ganji, S. H.; Tavintharan, S.; Zhu, D.; Xing, Y.; Kamanna, V. S.; Kashyap, M. L. Niacin
    Noncompetitively Inhibits DGAT2 but Not DGAT1 Activity in HepG2 Cells. *J. Lipid Res.*
    2004, *45* (10), 1835–1845.

(37) Lardizabal, K.; Effertz, R.; Levering, C.; Mai, J.; Pedroso, M. C.; Jury, T.; Aasen, E.;
    Gruys, K.; Bennett, K. Expression of Umbelopsis Ramanniana DGAT2A in Seed

506   Increases Oil in Soybean. *Plant Physiol.* **2008**, *148* (1), 89–96.

507 (38) Stoveken, T.; Kalscheuer, R.; Malkus, U.; Reichelt, R.; Steinbuchel, A.; Stöveken, T.;

508   Kalscheuer, R.; Malkus, U.; Reichelt, R.; Steinbüchel, A. The Wax Ester Synthase/Acyl

509   Coenzyme A:Diacylglycerol Acyltransferase from *Acinetobacter Sp*. Strain ADP1:

510   Characterization of a Novel Type of Acyltransferase. *J. Bacteriol.* **2005**, *187* (4), 1369–

511   1376.

512 (39) Daniel, J.; Deb, C.; Dubey, V. S.; Sirakova, T. D.; Abomoelak, B.; Morbidoni, H. R.;

513   Kolattukudy, P. E. Induction of a Novel Class of Diacylglycerol Acyltransferases and

514   Triacylglycerol Accumulation in *Mycobacterium Tuberculosis* as It Goes into a

515   Dormancy-Like State in Culture. *J. Bacteriol.* **2004**, *186* (15), 5017–5030.

516 (40) Elamin, A. A.; Stehr, M.; Spallek, R.; Rohde, M.; Singh, M. The *Mycobacterium*

517   *Tuberculosis* Ag85A Is a Novel Diacylglycerol Acyltransferase Involved in Lipid Body

518   Formation. *Mol. Microbiol.* **2011**, *81* (6), 1577–1592.

519 (41) McFie, P. J.; Banman, S. L.; Kary, S.; Stone, S. J. Murine Diacylglycerol Acyltransferase-

520   2 (DGAT2) Can Catalyze Triacylglycerol Synthesis and Promote Lipid Droplet Formation

521   Independent of Its Localization to the Endoplasmic Reticulum. *J. Biol. Chem.* **2011**, *286*

522   (32), 28235–28246.

523 (42) Jin, Y.; McFie, P. J.; Banman, S. L.; Brandt, C. J.; Stone, S. J. Diacylglycerol

524   Acyltransferase-2 (DGAT2) and Monoacylglycerol Acyltransferase-2 (MGAT2) Interact

525   to Promote Triacylglycerol Synthesis. *J. Biol. Chem.* **2014**, *289* (41), 28237–28248.

526 (43) Wei, H.; Shi, Y.; Ma, X.; Pan, Y., Hu, H.; Li, Y.; Luo, M.; Gerken, H.; Liu, J. A type-I

527   Diacylglycerol Acyltransferase Modulates Triacylglycerol Biosynthesis and Fatty Acid

24

528   Composition in the Oleaginous Microalga, *Nannochloropsis oceanica*. *Biotechnol.*

529   *Biofuels.* **2017**, *10*(1): 174.

530 (44) Cui, Y.; Zhao, J.; Wang, Y.; Qin, S.; Lu, Y. Characterization and Engineering of a Dual-

531   function Diacylglycerol Acyltransferase in the Oleaginous Marine Diatom *Phaeodactylum*

532   *tricornutum*. *Biotechnol. Biofuels*. **2018**, 11(1): 32.

533

FIGURE CAPTIONS

535 **Figure 1.** Sequence analyses of DGAT2s from *C. zofingiensis* and other organisms. Phylogenetic

536 relationship among deduced amino acid sequences of CzDGAT2s and DGAT2s from other

537 organisms is shown on the left, with the bootstrap values shown at the tree nodes. The gene

538 structure of each *DGAT2* is shown in the middle, with exons and introns represented by blue

539 boxes and black lines, respectively. * The gene structures of HsDGAT2 and MmDGAT2 are

540 shown in Supplementary Figure S2 due to their large gene sizes. The prediced transmembrane

541 domains of each deduced protein are shown on the right. The transmembrane domains were

542 predicted using TMHMM and are denoted by red boxes. The organisms and

543 Phytozome/Genbank accession number for each protein sequence are shown as follows:

544 *Arabidopsis thaliana*, At, AtDGAT2 (NP_566952); *Chlamydomonas reinhardtii,* Cre,

545 CreDGAT2A (Cre03.g205050), CreDGAT2B (Cre12.g557750), CreDGAT2C (Cre02.g079050),

546 CreDGAT2D (Cre06.g299050), CreDGAT2E (Cre09.g386912); *Homo sapiens*, *Hs*, HsDGAT2

547 (AAK84176); *Linum usitatissimum*, *Lu*, LuDGAT2 (KC437084); *Mus musculus*, *Mm*,

548 MmDGAT2 (AAK84175); *Saccharomyces cerevisiae,* Sc, ScDGAT2 (NP_014888).

549

550 **Figure 2.** Sequence logo and alignment of functional motifs of DGAT2s. The functional motifs

551 are shown in blue boxes, including a putative lipid binding motif. (A), FLXLXXXn; n, nonpolar

552 amino acid; (B) the "YFP" motif; (C) the "HPHG" motif; (D) the "RXGFX(K/ R)

553 XAXXXGXX(L/V)VPXXXFG(E/Q)" motif.

554

555 **Figure 3.** CzDGAT2C restored TAG synthesizing ability of yeast mutant H1246. (A) TLC

556 separation of yeast total lipids extracts. TAG STD, TAG standard. (B) TAG content (w/w, dry

557   weight) in yeast cells producing various CzDGAT2s. (C) TAG content (w/w, dry weight) in yeast

558   producing CzDGAT2C cultured in the presence of exogenous linoleic acid ($18:2\Delta^{9cis,12cis}$, C18:2),

559   α-linolenic acid ($C18:3\Delta^{9cis,12cis,18cis}$, C18:3Δ9), or γ-linolenic acid ($C18:3\Delta^{6cis,9cis,12cis}$, C18:3Δ6).

560   (D) Fatty acid composition (weight %) of TAG isolated from yeast producing CzDGAT2C

561   cultured in the presence of exogenous linoleic acid (C18:2). Yeast cells were harvested after 48 h

562   of induction for lipid analysis. FA, fatty acid; MUFA, monounsaturated fatty acids (C16:1 and

563   C18:1); SFA, saturated fatty acids (C16:0 and C18:0). Data represent mean ± S.D., n=3.

564

565   **Figure 4.** *In vitro* DGAT assay using yeast microsomal fractions containing recombinant

566   CzDGAT2C. (A) Enzyme activity of CzDGAT2C. (B) CzDGAT2C activity in response to

567   increasing acyl-CoA concentrations. Enzyme activity data were fitted to a nonlinear regression

568   using Michaelis–Menten equation ($R^2 = 0.93$). Plots were generated using GraphPad Prism. (C)

569   A predicted transmembrane topology of CzDGAT2C by TMHMM. (D) Truncation mutagenesis

570   of CzDGAT2C. Data represent mean ± S.D., n=3.

571

572   **Figure 5.** Possible physical interactions among CzDGAT2s. Protein-protein interaction between

573   CzDGAT2s were tested using split-ubiquitin membrane yeast two-hybrid assays. cDNA

574   encoding each CzDGAT2 was ligated to the Lex A - C-terminal fragment of ubiquitin (Cub) and

575   the N-terminal fragment of ubiquitin containing an Ile/Gly point mutation (NubG), yielding C_{ub}-

576   bait and $N_{ub}G$-prey, respectively. Serial dilutions of yeast cells co-transformed with each

577   bait/prey combination were spotted on synthetic drop-out (SD) agar plates lacking Ade, His, Leu
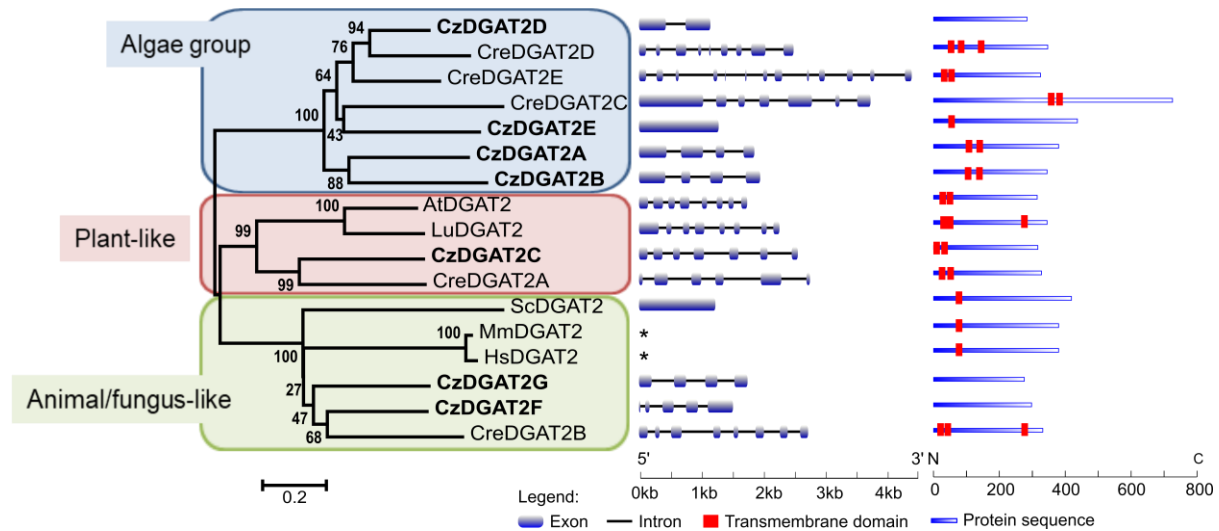
578   and Trp (SD-A-H-L-T).

Figure 1. Sequence analyses of DGAT2s from *C. zofingiensis* and other organisms. Phylogenetic relationship among deduced amino acid sequences of CzDGAT2s and DGAT2s from other organisms is shown on the left, with the bootstrap values shown at the tree nodes. The gene structure of each *DGAT2* is shown in the middle, with exons and introns represented by blue boxes and black lines, respectively. * The gene structures of HsDGAT2 and MmDGAT2 are shown in Supplementary Figure S2 due to their large gene sizes. The prediced transmembrane domains of each deduced protein are shown on the right. The transmembrane domains were predicted using TMHMM and are denoted by red boxes. The organisms and Phytozome/Genbank accession number for each protein sequence are shown as follows: *Arabidopsis thaliana*, At, AtDGAT2 (NP_566952); *Chlamydomonas reinhardtii,* Cre, CreDGAT2A (Cre03.g205050), CreDGAT2B (Cre12.g557750), CreDGAT2C (Cre02.g079050), CreDGAT2D (Cre06.g299050), CreDGAT2E (Cre09.g386912); *Homo sapiens*, *Hs*, HsDGAT2 (AAK84176); *Linum usitatissimum*, *Lu*, LuDGAT2 (KC437084); *Mus musculus*, *Mm*,

MmDGAT2 (AAK84175); *Saccharomyces cerevisiae,* Sc, ScDGAT2 (NP_014888).
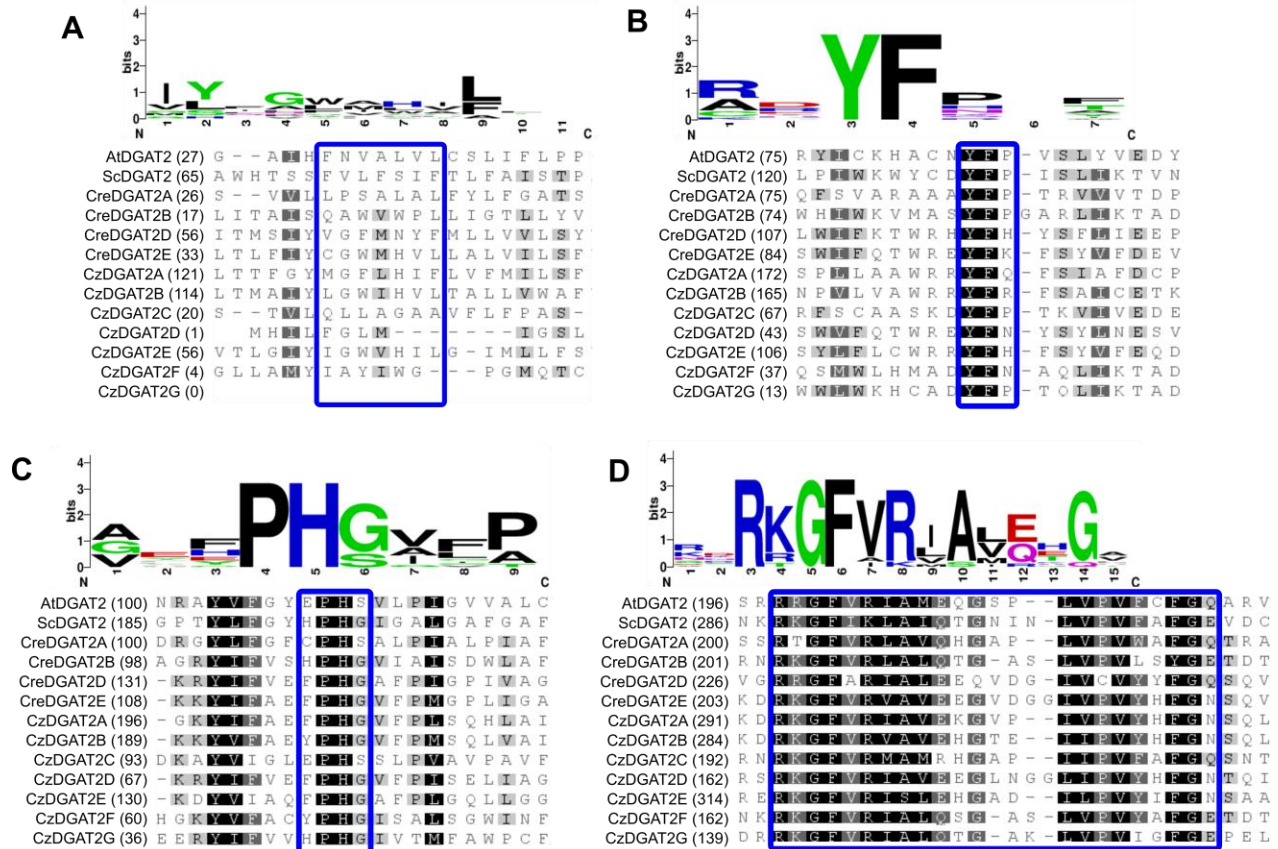
Figure 2. Sequence logo and alignment of functional motifs of DGAT2s. The functional motifs are shown in blue boxes, including a putative lipid binding motif. (A), FLXLXXXn; n, nonpolar amino acid; (B) the "YFP" motif; (C) the "HPHG" motif; (D) the "RXGFX(K/R) XAXXXGXX(L/V)VPXXXFG(E/Q)" motif.
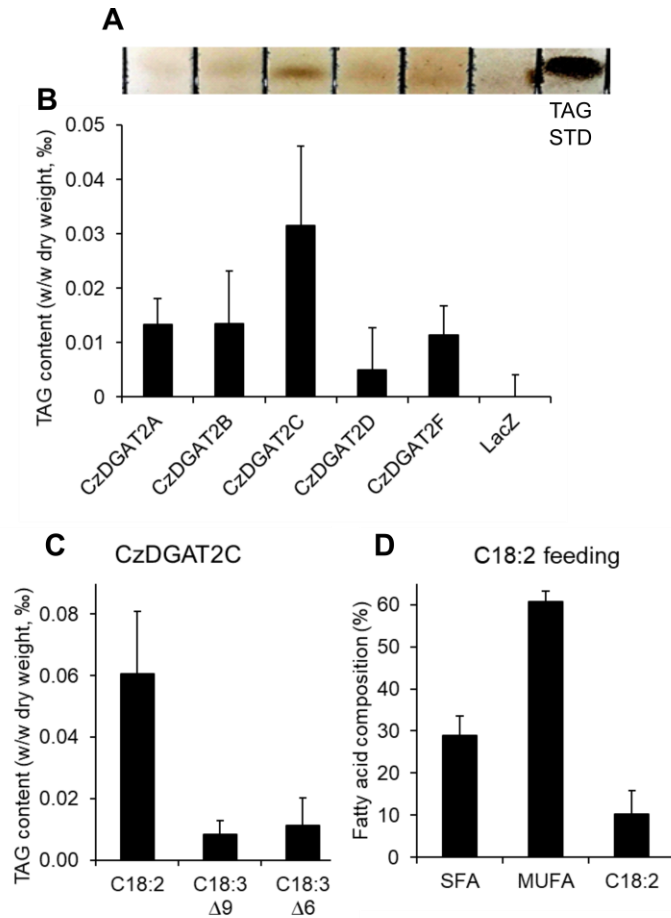
Figure 3. CzDGAT2C restored TAG synthesizing ability of yeast mutant H1246. (A) TLC separation of yeast total lipids extracts. TAG STD, TAG standard. (B) TAG content (w/w, dry weight) in yeast cells producing various CzDGAT2s. (C) TAG content (w/w, dry weight) in yeast producing CzDGAT2C cultured in the presence of exogenous linoleic acid ($18:2\Delta^{9cis,12cis}$, C18:2), α-linolenic acid ($C18:3\Delta^{9cis,12cis,18cis}$, C18:3Δ9), or γ-linolenic acid ($C18:3\Delta^{6cis,9cis,12cis}$, C18:3Δ6). (D) Fatty acid composition (weight %) of TAG isolated from yeast producing CzDGAT2C cultured in the presence of exogenous linoleic acid (C18:2). Yeast cells were harvested after 48 h of induction for lipid analysis. FA, fatty acid; MUFA, monounsaturated fatty acids (C16:1 and C18:1); SFA, saturated fatty acids (C16:0 and C18:0). Data represent mean ± S.D., n=3.
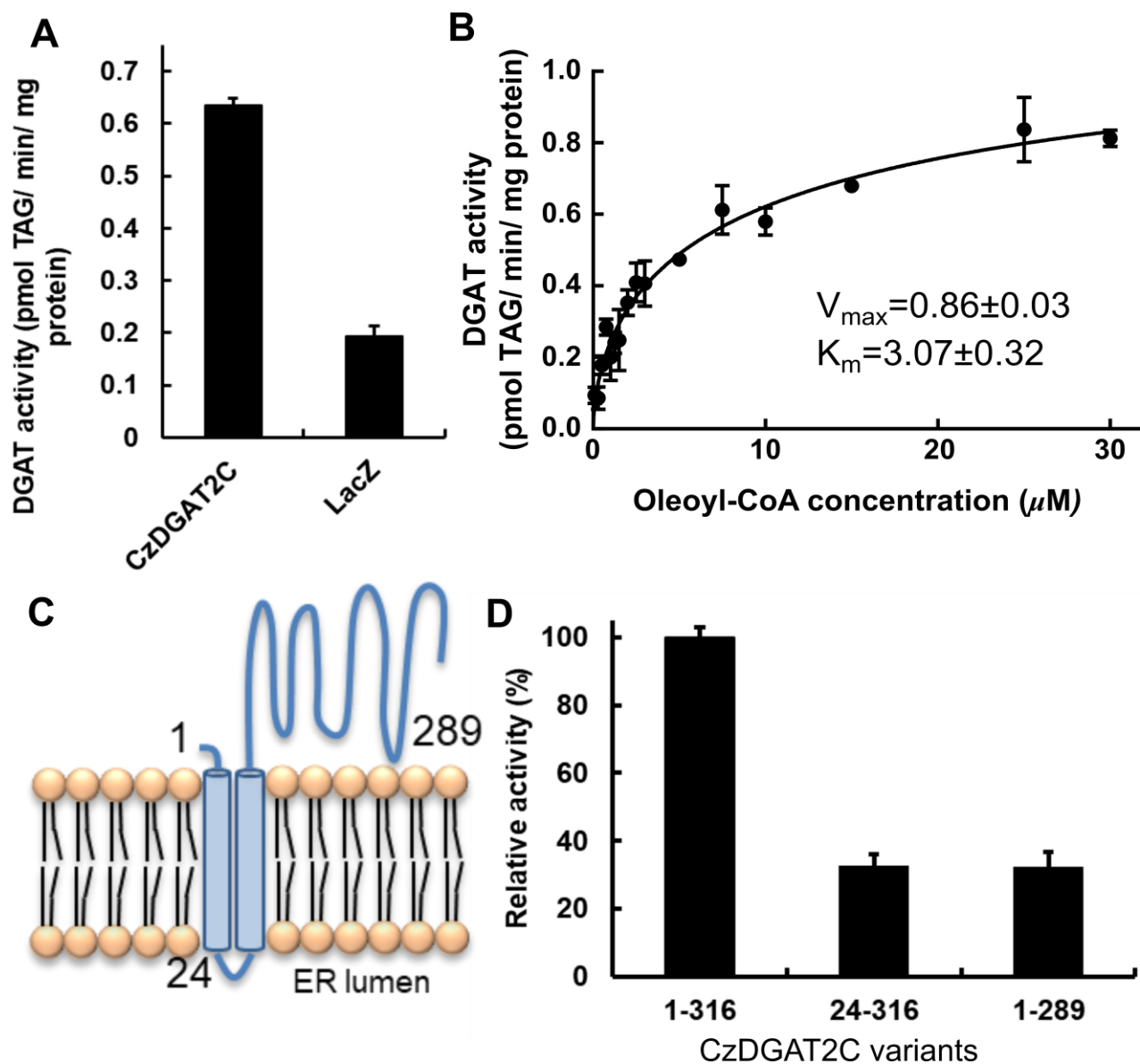
Figure 4. *In vitro* DGAT assay using yeast microsomal fractions containing recombinant CzDGAT2C. (A) Enzyme activity of CzDGAT2C. (B) CzDGAT2C activity in response to increasing acyl-CoA concentrations. Enzyme activity data were fitted to a nonlinear regression using Michaelis–Menten equation ($R^2 = 0.93$). Plots were generated using GraphPad Prism. (C) A predicted transmembrane topology of CzDGAT2C by TMHMM. (D) Truncation mutagenesis of CzDGAT2C. Data represent mean ± S.D., n=3.
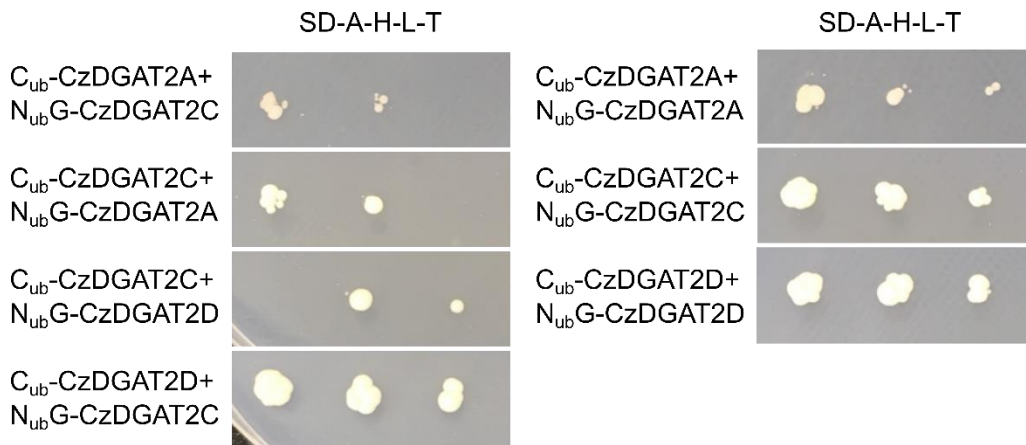
Figure 5. Possible physical interactions among CzDGAT2s. Protein-protein interaction between CzDGAT2s were tested using split-ubiquitin membrane yeast two-hybrid assays. cDNA encoding each CzDGAT2 was ligated to the Lex A - C-terminal fragment of ubiquitin (Cub) and the N-terminal fragment of ubiquitin containing an Ile/Gly point mutation (NubG), yielding C_{ub}-bait and N_{ub}G-prey, respectively. Serial dilutions of yeast cells co-transformed with each bait/prey combination were spotted on synthetic drop-out (SD) agar plates lacking Ade, His, Leu and Trp (SD-A-H-L-T).

Graphic for Table of Contents Only